

# Novel Platinum–Ruthenium Dinuclear Complex Bridged by 2-Aminoethanethiol

Rei Okamura, Tohru Wada, and Koji Tanaka\*

Institute for Molecular Science, and CREST, Japan Science and Technology Agency (JST),  
5-1 Higashiyama, Myodaiji, Okazaki 444-8787

Received April 6, 2006; E-mail: ktanaka@ims.ac.jp

A platinum–ruthenium dinuclear complex,  $[(\text{PtCl})\{\text{RuCl}(\text{Bu}_2\text{sq})\}(\text{btpyxa})]^{2+}$  ( $[2]^{2+}$ ) ( $\text{btpyxa}$  = 2,7-di-*tert*-butyl-9,9-dimethyl-4,5-bis(2,2':6',2''-terpyrid-4'-yl)xanthene,  $\text{Bu}_2\text{sq}$  = 3,5-di-*tert*-butyl-1,2-benzosemiquinonate ion), in which  $\text{btpyxa}$  acts as a bridging ligand, was prepared, and its physical properties were compared to those of an analogous dmsO complex,  $[(\text{PtCl})\{\text{Ru}(\text{Bu}_2\text{sq})(\text{dmsO})\}(\text{btpyxa})]^{2+}$  ( $[1]^{2+}$ ) ( $\text{dmsO}$  = dimethyl sulfoxide). Treatment of complex  $[1]^{2+}$  with an aqueous NaOH solution followed by 2-aminoethanethiol afforded  $[(\text{Pt}(\text{SCH}_2\text{CH}_2\text{NH}_2))\{\text{Ru}(\text{Bu}_2\text{sq})(\text{dmsO})\}(\text{btpyxa})]^{2+}$  ( $[3]^{2+}$ ). On the other hand, the reaction of complex  $[2]^{2+}$  with 2-aminoethanethiol produced  $[(\text{Pt}(\text{SCH}_2\text{CH}_2\text{NH}_2)\text{Ru}(\text{Bu}_2\text{sq}))(\text{btpyxa})]^{2+}$  ( $[4]^{2+}$ ), in which Pt and Ru atoms are bridged by the 2-aminoethanethiolato ligand. Complex  $[4]^{2+}$  was also obtained by heating complex  $[3]^{2+}$  in 2-methoxyethanol.

Metal–dioxolene complexes have attracted much attention from the viewpoints of not only their characteristic metal-centered and ligand-localized redox reactions but also charge-distributions over the central metal and the ligand depending on the oxidation states of the two redox sites.<sup>1</sup> We have been studying ruthenium–dioxolene complexes bearing polypyridine as an ancillary ligand to develop new redox catalysts utilizing their characteristic redox reactions.<sup>2</sup> An unprecedented oxyl radical complex,  $[\text{Ru}^{\text{II}}(\text{Bu}_2\text{sq})(\text{O}^{\bullet-})(\text{terpy})]^{0+}$ , is formed through double deprotonation of aqua protons of  $[\text{Ru}^{\text{III}}(\text{Bu}_2\text{sq})(\text{OH}_2)(\text{terpy})]^{2+}$  ( $\text{Bu}_2\text{sq}$  = 3,5-di-*tert*-butyl-1,2-benzosemiquinonate ion,  $\text{terpy}$  = 2,2':6',2''-terpyridine) which is coupled with intramolecular electron transfer from the resultant negatively charged oxo ligand to the metal center.<sup>3</sup> Moreover, a coupling reaction between two oxyl radical groups that were generated through deprotonation of two hydroxy groups of a bis(hydroxo-ruthenium–dioxolene) framework, in which two hydroxo groups were located inside of the cavity formed by two ruthenium–dioxolene units and a bridging ligand, enabled smooth catalytic four-electron oxidation of water under the controlled potential electrolysis in water.<sup>4</sup> On the other hand, a platinum–ruthenium heterodinuclear complex,  $[(\text{PtCl})\{\text{Ru}(\text{Bu}_2\text{sq})(\text{dmsO})\}(\text{btpyxa})]^{2+}$  ( $[1]^{2+}$ ) having a flexible  $\text{btpyxa}$  bridging ligand ( $\text{btpyxa}$  = 2,7-di-*tert*-butyl-9,9-dimethyl-4,5-bis(2,2':6',2''-terpyrid-4'-yl)xanthene)<sup>5</sup> which was synthesized for the purpose of activating organic molecules and water via the Pt and Ru ions, respectively, showed no electronic interaction between the Pt( $\text{terpy}$ ) group and  $\text{Ru}(\text{Bu}_2\text{sq})$  one.<sup>5</sup> We, therefore, introduced 2-aminoethanethiol as a bridging ligand to promote electronic interaction between the two metal ions considering not only the strong affinity of Pt toward thiolato ligands but also the arrangement of coordination sites on both metal centers to induce electronic interactions between the two reaction sites. Herein, we discuss the novel platinum–ruthenium complex  $[(\text{PtCl})\{\text{RuCl}(\text{Bu}_2\text{sq})\}(\text{btpyxa})]^{2+}$  ( $[2]^{2+}$ ) and the reactions of complex  $[1]^{2+}$  and  $[2]^{2+}$  with 2-aminoethanethiol (Fig. 1).

## Results and Discussion

**Synthesis and Characterization of  $[(\text{PtCl})\{\text{RuCl}(\text{Bu}_2\text{sq})\}(\text{btpyxa})]^{2+}$  ( $[2]^{2+}$ ).** The hetero-dinuclear complex  $[(\text{PtCl})(\text{RuCl}_3)(\text{btpyxa})](\text{OTf})$  was prepared by the reaction of  $[(\text{PtCl})(\text{btpyxa})](\text{OTf})^5$  with  $\text{RuCl}_3 \cdot 3\text{H}_2\text{O}$  in EtOH. A dark brown methanolic suspension of  $[(\text{PtCl})(\text{RuCl}_3)(\text{btpyxa})](\text{OTf})$  gradually changed to a homogeneous purple solution after an addition of potassium 3,5-di-*tert*-butylcatecholate. Crude products obtained by evaporation of the solvent were chromatographed over alumina using an acetone/EtOH (5/1) as an eluent and a violet solution was collected.  $[\text{Fe}(\text{C}_5\text{H}_5)_2](\text{PF}_6)$ , used

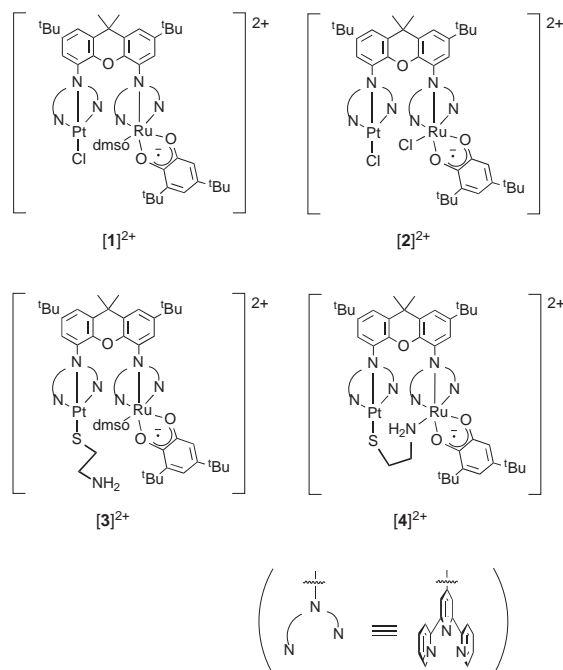


Fig. 1. Platinum–ruthenium dinuclear complexes in this study.

as an oxidant, was added to the violet solution followed by the addition of an aqueous  $\text{NH}_4\text{PF}_6$  to the solution afforded  $[(\text{PtCl})\{\text{RuCl}(\text{Bu}_2\text{sq})\}(\text{btpyxa})](\text{PF}_6)_2$  (**[2]**)( $\text{PF}_6$ )<sub>2</sub> as a dark-blue powder. In the ESI-MS spectrum, complex **[2]**<sup>2+</sup> was observed as  $\text{M}^{2+}$  at  $m/z = 686$ .

In the cyclic voltammogram (CV) of complex **[2]**<sup>2+</sup> in  $\text{CH}_2\text{Cl}_2$ , a strong cathodic wave at  $E_{\text{pc}} = -0.70$  V in the cathodic potential sweep, two anodic waves at  $E_{\text{pa}} = -0.61$  and  $-0.41$  V in the reverse scan, and a reversible redox couple at  $E_{1/2} = +0.17$  V were observed (Fig. 2a, Table 1).

Because  $[\text{RuCl}(\text{Bu}_2\text{sq})(\text{terpy})]^{2+}$  shows semiquinone/catecholate and  $\text{Ru}^{\text{II}}/\text{Ru}^{\text{III}}$  redox couples at  $E_{1/2} = -0.73$  V

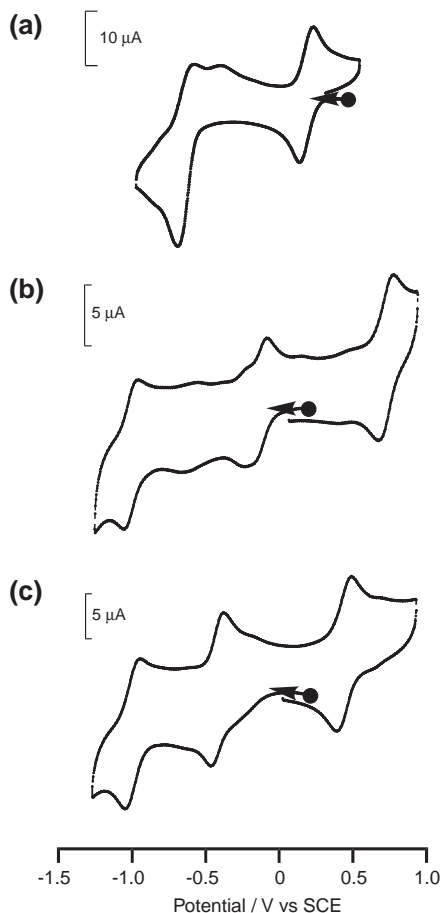


Fig. 2. Cyclic voltammograms of complexes (a) **[2]**<sup>2+</sup> (1.0 mM), (b) **[3]**<sup>2+</sup> (1.0 mM), and (c) **[4]**<sup>2+</sup> (1.0 mM) in  $\text{CH}_2\text{Cl}_2$  containing 0.1 M  $n\text{Bu}_4\text{NPF}_6$ . The dot in the voltammograms is the equilibrium electrode potential of the solutions.

and  $E_{1/2} = +0.16$  V, respectively, and reduction of the  $\text{Pt}^{\text{II}}(\text{btpyxa})$  framework in  $[(\text{PtCl})(\text{btpyxa})]^+$  took place at  $E_{1/2} = -0.78$  V,<sup>5</sup> the redox reaction at  $E_{1/2} = +0.17$  V was assigned to the  $\text{Ru}^{\text{II}}/\text{Ru}^{\text{III}}$  couple. The strong cathodic wave at  $E_{\text{pc}} = -0.70$  V and the two anodic waves at  $E_{\text{pa}} = -0.61$  and  $-0.41$  V of **[2]**<sup>2+</sup>, therefore, result from the summation of the redox reactions of the dioxolene ligand and the platinum–terpyridyl frameworks. The large cathodic shift of the  $\text{Ru}^{\text{II}}/\text{Ru}^{\text{III}}$  redox potential of complex **[2]**<sup>2+</sup> compared with that of complex **[1]**<sup>2+</sup> ( $E_{1/2} = +0.64$  V) is associated with the  $\pi$ -acceptor character of *S*-bound dmsol of the latter and the  $\sigma$ -donor one of  $\text{Cl}^-$  of the former. Thus, the redox behavior of complex **[2]**<sup>2+</sup> is close to the summation of the redox reactions of both  $[\text{Pt}^{\text{II}}\text{Cl}(\text{terpy})]^+$  and  $[\text{Ru}^{\text{III}}\text{Cl}(\text{Bu}_2\text{sq})(\text{terpy})]^+$ . Indeed, EPR spectra of complex **[2]**<sup>2+</sup> did not display any signals due to antiferromagnetic coupling between  $\text{Ru}^{\text{III}}$  and semiquinone.

The electronic spectra of Ru–dioxolene complexes reflect their electronic structures, since the  $\text{Ru}^{\text{II}}$ –semiquinone (or  $\text{Ru}^{\text{III}}$ –catecholate) and  $\text{Ru}^{\text{III}}$ –semiquinone (or  $\text{Ru}^{\text{II}}$ –quinone) frameworks show characteristic absorption bands around 800 and 600 nm, respectively. In accordance with this, complex **[2]**<sup>2+</sup> in  $\text{CH}_2\text{Cl}_2$  (Fig. 3a, Table 2) showed a strong CT band at 605 nm ( $\epsilon$  18100  $\text{M}^{-1}\text{cm}^{-1}$ ) similar to that of  $[\text{Ru}^{\text{III}}(\text{OH}_2)(\text{Bu}_2\text{sq})(\text{terpy})]$  (600 nm).<sup>3</sup>

The band at 605 nm completely disappeared upon electrochemical reduction of the complex at  $-0.1$  V, whereas a new band appeared at 876 nm assigned to the CT band within the  $\text{Ru}^{\text{II}}$ –semiquinonate framework.<sup>2a</sup> Further electrochemical reduction of the resultant complex **[2]**<sup>+</sup> at  $-1.0$  V caused the 876 nm band to disappear due to the formation of complex **[2]**<sup>0</sup> bearing a  $\text{Ru}^{\text{II}}$ –catecholate core, which has no CT transition bands in the visible region. Oxidation of complex **[2]**<sup>0</sup> at  $+0.3$  V regenerated the original absorption spectrum of complex **[2]**<sup>2+</sup>.

#### Reaction of Pt–Ru Complexes with 2-Aminoethanethiol.

Many attempts to obtain single crystals of complexes **[1]**<sup>2+</sup> and **[2]**<sup>2+</sup> for the X-ray analyses were unsuccessful. The atomic distance between Pt and Ru in the dinuclear complexes is reasonably deduced based on the molecular structure of  $[(\text{PtCl})(\text{btpyxa})]^+$ , in which the two terpyridyl planes are separated by 4.1 to 4.7 Å.<sup>5</sup> Removal of Cl and dmsol ligated on Pt and Ru ions, therefore, is expected to provide a wide space enough for the activation of small molecules on the two metal centers. Taking into consideration not only the strong affinity of Pt toward thiolato ligand but also the roughly orthogonal arrangement of the Pt–Cl and Ru–Cl bonds in complex **[2]**<sup>2+</sup> (see Fig. 1), 2-aminoethanethiol was used as a model substrate

Table 1. CV Data of the Complexes in  $\text{CH}_2\text{Cl}_2$

Complexes	$E_{1/2}/\text{V vs SCE}$		
	$\text{Ru}^{\text{III}}/\text{Ru}^{\text{II}}$	sq/cat	$\text{Pt}(\text{terpy})/\text{Pt}(\text{terpy}^-)$
<b>[1]</b> <sup>2+</sup> <sup>5</sup>	+0.64	−0.33	−0.74
<b>[2]</b> <sup>2+</sup>	+0.17	−0.41 ( $E_{\text{pa}}$ ), −0.61 ( $E_{\text{pa}}$ ), −0.70 ( $E_{\text{pc}}$ )	—
<b>[3]</b> <sup>2+</sup>	+0.71	−0.17	−1.01
<b>[4]</b> <sup>2+</sup>	+0.44	−0.42	−0.99
$[\text{Ru}^{\text{II}}\text{Cl}(\text{Bu}_2\text{sq})(\text{terpy})]^{2+}$	+0.16	−0.73	—
$[(\text{PtCl})(\text{btpyxa})]^+$ <sup>5</sup>	—	—	−0.78

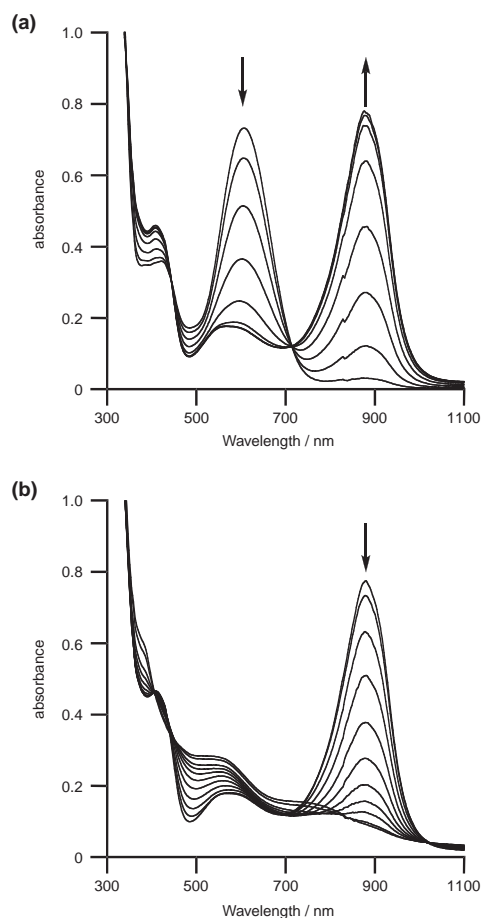


Fig. 3. Absorption spectral change of complex  $[2]^{2+}$  ( $1.0 \text{ mM}$ ) in  $\text{CH}_2\text{Cl}_2$  containing  $0.1 \text{ M } n\text{-Bu}_4\text{NPF}_6$  at  $-0.1 \text{ V}$  (a) and at  $-1.0 \text{ V}$  (b). The arrows in the figures indicate the direction of the changes of the spectra.

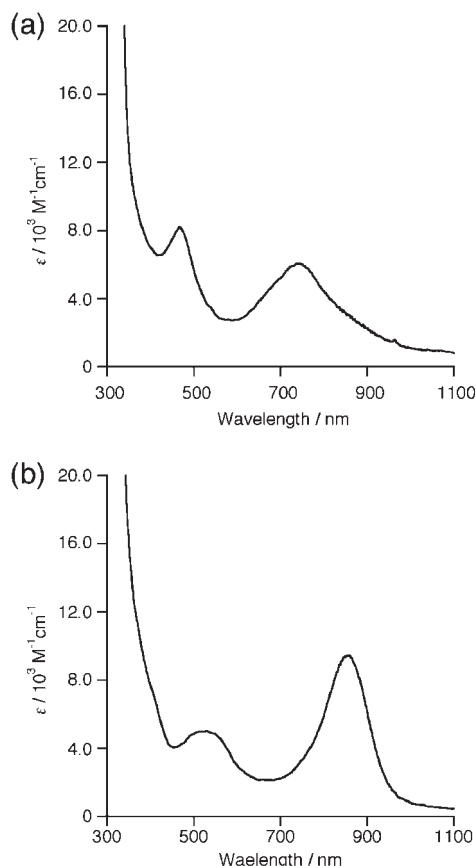


Fig. 4. UV-vis-NIR spectra of complexes  $[3]^{2+}$  (a) and  $[4]^{2+}$  (b) in  $\text{CH}_2\text{Cl}_2$ .

Table 2. UV-Vis-NIR Spectral Data of the Complexes in  $\text{CH}_2\text{Cl}_2$

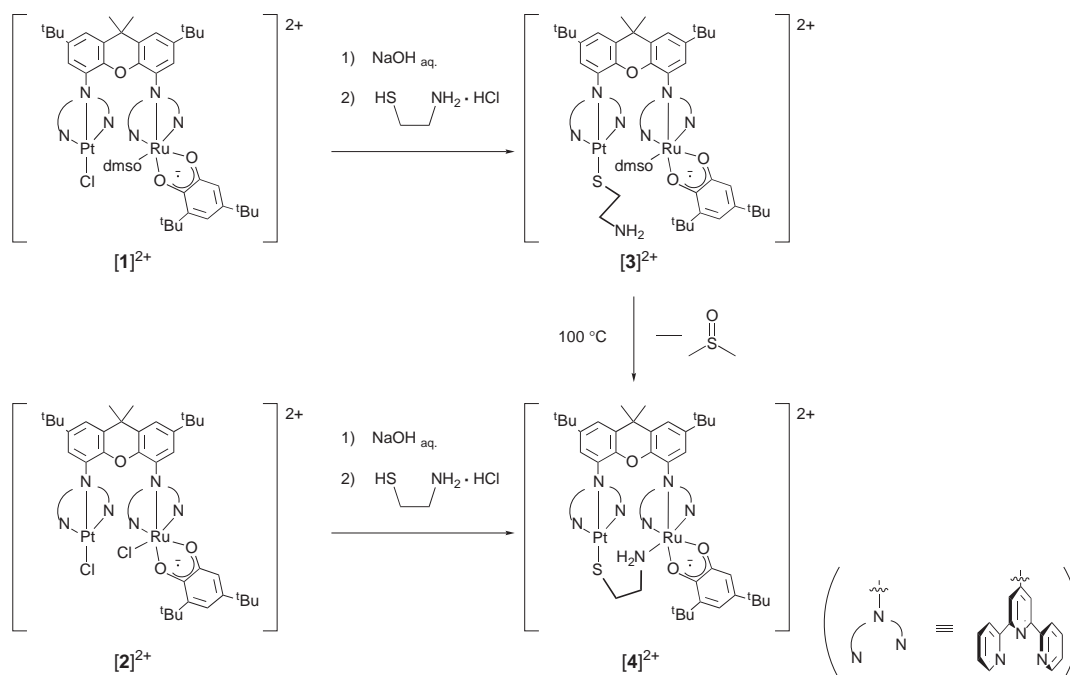
Complexes	$\lambda_{\text{max}}/\text{nm}$ ( $\epsilon/10^3 \text{ M}^{-1} \text{ cm}^{-1}$ )
$[1]^{2+5}$	273(52.2), 284(52.3), 308(43.5), 421(8.1), 742(6.2)
$[2]^{2+}$	264(56.8), 285(54.5), 422(8.7), 605(18.1)
$[3]^{2+}$	277(53.8), 309(48.5), 467(7.7), 743(6.0)
$[4]^{2+}$	278(54.2), 316(41.4), 520(5.1), 857(9.4)
$[\text{Ru}^{\text{II}}\text{Cl}(\text{tBu}_2\text{sq})(\text{terpy})]^{2a}$	238(33.9), 280(24.0), 318(25.1), 370(6.0), 584(4.1), 876(19.0)
$[\text{Ru}^{\text{II}}(\text{tBu}_2\text{sq})(\text{dmsO})(\text{terpy})]^{+5}$	271(24.1), 308(35.4), 457(5.1), 737(7.5)

with the aim to active small molecules on the two metal centers. Treatment of a 2-methoxyethanol solution of complex  $[1]^{2+}$  with an excess amount of an aqueous NaOH solution followed by the subsequent addition of 1 equiv of 2-aminoethanethiol to the solution produced  $[\{\text{Pt}(\text{SCH}_2\text{CH}_2\text{NH}_2)\}\{\text{Ru}(\text{tBu}_2\text{sq})(\text{dmsO})(\text{btpyxa})\}]^{2+}$  ( $[3]^{2+}$ ) in a relatively high yield. In the ESI-MS spectrum of the complex, obtained as a  $\text{PF}_6$  salt, the dication parent peak at  $m/z$  728, which corresponds to the molecular formula  $[\{\text{Pt}(\text{SCH}_2\text{CH}_2\text{NH}_2)\}\{\text{Ru}(\text{tBu}_2\text{sq})(\text{dmsO})(\text{btpyxa})\}]^{2+}$ , was observed. The UV-vis-NIR spectrum of complex  $[3]^{2+}$  in  $\text{CH}_2\text{Cl}_2$  (Fig. 4a, Table 2) had two broad bands at 743 nm ( $\epsilon$   $6000 \text{ M}^{-1} \text{ cm}^{-1}$ ) and 467 nm ( $\epsilon$   $7700 \text{ M}^{-1} \text{ cm}^{-1}$ ) which were assigned to the CT bands of the  $\text{Ru}^{\text{II}}$ -semiquinone and  $\text{Ru}^{\text{II}}$ -terpyridyl frameworks, respectively, based

on those of  $[\text{Ru}(\text{tBu}_2\text{sq})(\text{dmsO})(\text{terpy})]^{+}$  ( $\lambda_{\text{max}} = 737$  and  $457 \text{ nm}$ ).<sup>5</sup>

$[\text{Pt}(\text{SCH}_2\text{CH}_2\text{OH})(\text{terpy})]^{+}$ ,<sup>6</sup>  $[\text{Pt}(\text{SAr})(\text{terpy})]^{+}$  (Ar = pyridyl, pyrimidyl, and quinolyl),<sup>7</sup>  $[\{\text{Pt}(\text{terpy})\}_2(\text{SArS})]^{2+}$  (Ar = xylyl),<sup>8</sup> and  $[\text{Pt}(\text{diimine})(\text{dithiolate})]^{9,10}$  have the weak CT band arising from Pt-thiolate bond between 400 and 600 nm. The strong MLCT band at 467 nm of complex  $[3]^{2+}$ , therefore, appears to obscure the CT band of the  $\text{Pt}(\text{SCH}_2\text{CH}_2\text{NH}_2)(\text{terpy})$  framework.

The CV of complex  $[3]^{2+}$  in  $\text{CH}_2\text{Cl}_2$  shows three redox couples at  $E_{1/2} = -1.01$ ,  $-0.17$ , and  $+0.71 \text{ V}$  (Fig. 2b, Table 1). The large cathodic shift in the redox potential of the platinum-terpyridyl moiety ( $E_{1/2} = -1.01 \text{ V}$ ) compared to that of the terpyridyl-platinum-chloride moiety in complex  $[1]^{2+}$

Scheme 1. The conversion from complexes  $[1]^{2+}$  and  $[2]^{2+}$  to complex  $[4]^{2+}$ .

( $E_{1/2} = -0.74$  V) is ascribed to the strong electron donor ability of the thiolato ligand. On the other hand, the redox potential of the  $\text{Ru}^{\text{II}}/\text{Ru}^{\text{III}}$  couple ( $E_{1/2} = +0.71$  V) and the UV–vis absorption spectrum of complex  $[3]^{2+}$  are quite close to those of complex  $[1]^{2+}$  ( $+0.64$  V) and  $[\text{Ru}(\text{Bu}_2\text{sq})(\text{dmsq})(\text{terpy})]^+$  ( $+0.65$  V).<sup>5</sup> In other words, there is little electronic interaction between the Pt site and the ruthenium–dioxolene–dmsq framework in these Pt–Ru dinuclear complexes.

Treatment of complex  $[2]^{2+}$  with excess amounts of base, followed by the reaction with 2-aminoethanethiol at ambient temperature gave  $[(\text{Pt}(\text{SCH}_2\text{CH}_2\text{NH}_2)\text{Ru}(\text{Bu}_2\text{sq}))(\text{btpyxa})]^{2+}$  ( $[4]^{2+}$ ), of which the parent peak appears at  $m/z$  689 a dicationic pattern in the ESI-MS spectrum. The 2-aminoethanethiolato group is stably coordinated to both the Pt ion and Ru ion in complex  $[4]^{2+}$  in a bridging mode, since the complex did not react with a 10-fold excess of DMSO or LiCl. The UV–vis–NIR spectrum of complex  $[4]^{2+}$  in  $\text{CH}_2\text{Cl}_2$  showed two bands at 857 nm ( $\epsilon$  9400  $\text{M}^{-1}\text{cm}^{-1}$ ) and around 520 nm ( $\epsilon$  5100  $\text{M}^{-1}\text{cm}^{-1}$ ) which were assigned to the CT bands resulting from the  $\text{Ru}^{\text{II}}$ –semiquinone and  $\text{Ru}^{\text{II}}$ – and/or  $\text{Pt}^{\text{II}}$ –terpyridine framework, respectively (Fig. 4b and Table 2). In addition, the similarities between both the UV–vis–NIR spectra and CV of complex  $[4]^{2+}$  and those of  $[\text{Ru}^{\text{II}}(\text{NH}_3)(\text{Bu}_2\text{sq})(\text{terpy})](\text{ClO}_4)_2^{\text{f}}$  also support the coordination of 2-aminoethanethiol to ruthenium via the amino group. Thus, the  $\text{Ru}^{\text{III}}$  ion in complex  $[2]^{2+}$  was reduced to  $\text{Ru}^{\text{II}}$  during the formation of complex  $[4]^{2+}$  under basic conditions. The pattern of CV of complex  $[4]^{2+}$  in  $\text{CH}_2\text{Cl}_2$  was different from that of complex  $[2]^{2+}$ . Three reversible redox waves at  $E_{1/2} = -0.99$ ,  $-0.42$ , and  $+0.44$  V are assigned to the terpyridyl–platinum–thiolate, catecholate/semiquinonate, and ruthenium-centered redox reactions, respectively (Fig. 2c, Table 1).

Complex  $[1]^{2+}$  was quite stable in solution. In addition, it did not undergo substitution of the dmsq ligand with free 2-aminoethanethiol in 2-methoxyethanol at 100 °C. On the other

hand, complex  $[4]^{2+}$  was obtained in a 76% yield through the substitution of the dmsq of complex  $[3]^{2+}$  by the terminal amino group of 2-aminoethanethiolate linked to the Pt atom. The conversions from complexes  $[1]^{2+}$  to  $[4]^{2+}$  through complex  $[3]^{2+}$  and from complexes  $[2]^{2+}$  to  $[4]^{2+}$  are summarized in Scheme 1.

Thus, the platinum site in complex  $[3]^{2+}$  has the function of arranging the 2-aminoethanethiol in the appropriate position in order to substitute the dmsq coordinated to the Ru ion, which is the redox center in the hetero-dinuclear platinum–ruthenium framework.

## Experimental

**Materials.** Commercially available  $\text{RuCl}_3 \cdot 3\text{H}_2\text{O}$  and 2-aminoethanethiol hydrochloride were used without further purification. The tetrabutylammonium hexafluorophosphate used as a supporting electrolyte for electrochemistry was recrystallized from hot ethanol. Ferrocenium hexafluorophosphate was synthesized by literature method.<sup>11</sup> Complexes  $[(\text{PtCl})(\text{btpyxa})](\text{OTf})$  and  $[(\text{PtCl})\{\text{Ru}(\text{Bu}_2\text{sq})(\text{dmsq})\}(\text{btpyxa})](\text{PF}_6)_2$  ( $[1](\text{PF}_6)_2$ ) were prepared as described previously.<sup>5</sup>

**Syntheses of the Complexes.**  **$[(\text{PtCl})(\text{RuCl}_3)(\text{btpyxa})](\text{OTf})$ :** A mixture of  $[(\text{PtCl})(\text{btpyxa})](\text{OTf})$  (93.4 mg, 0.080 mmol) and  $\text{RuCl}_3 \cdot 3\text{H}_2\text{O}$  (32.9 mg, 0.126 mmol) suspended in ethanol (20 mL) was refluxed with stirring for 14 h under  $\text{N}_2$ . The dark-brown solid which precipitated was separated by centrifugation. The product thus obtained was washed with water and dried in vacuo. Yield: 89.1 mg (0.063 mmol, 79%). Anal. Calcd for  $\text{C}_{54}\text{H}_{48}\text{Cl}_4\text{F}_3\text{N}_6\text{O}_4\text{PtRuS} \cdot 2\text{H}_2\text{O}$ : C, 46.06; H, 3.72; N, 5.97%. Found: C, 46.11; H, 4.03; N, 6.06%. ESI-MS:  $m/z$  593 ( $[(\text{PtCl})(\text{RuCl}_2)(\text{btpyxa})]^{2+}$ ).

**$[(\text{PtCl})\{\text{RuCl}(\text{Bu}_2\text{sq})\}(\text{btpyxa})](\text{PF}_6)_2$  ( $[2](\text{PF}_6)_2$ ):** A methanolic solution (30 mL) of potassium *tert*-butoxide (17.5 mg, 0.156 mmol) was added to a methanolic suspension (50 mL) of 3,5-di-*tert*-butylcatechol (17.4 mg, 0.078 mmol) and  $[(\text{PtCl})(\text{RuCl}_3)(\text{btpyxa})](\text{OTf})$  (107.0 mg, 0.078 mmol), and then the mix-



ture was stirred at room temperature for 14 h under  $N_2$ . The resulting dark purple solution was evaporated to dryness under reduced pressure. The residue was dissolved in a small amount of acetone and chromatographed over an Alumina A-Super I column (ICN Biomedicals GmbH). A dark-blue band containing a mixture of complexes  $[2]^+$  and  $[2]^{2+}$  eluted with acetone/EtOH (5/1) was collected and the solvent was evaporated. To a methanol solution (20 mL) of the residue was added  $[Fe(C_5H_5)_2](PF_6)$  (25.9 mg, 0.078 mmol), and the mixture was stirred at room temperature for 14 h under  $N_2$ . The resulting dark-blue solution was evaporated to dryness and purification by column chromatography was repeated. A dark-blue band of complex  $[2]^{2+}$  eluted with  $CH_2Cl_2$ /acetone (1/1) was collected and evaporated to dryness under reduced pressure. Addition of a saturated aqueous solution of  $NH_4PF_6$  to the methanol solution resulted in precipitation of a dark-blue solid, which was separated by centrifugation, washed with water and dried in vacuo. Yield: 61.3 mg (0.037 mmol, 47%). Anal. Calcd for  $C_{67}H_{68}Cl_2F_{12}N_6O_3P_2PtRuS \cdot 2H_2O$ : C, 47.38; H, 4.27; N, 4.95%. Found: C, 47.42; H, 4.39; N, 4.89%. ESI-MS:  $m/z$  686 ( $[PtCl\{RuCl(Bu_2sq)\}(btpyxa)]^{2+}$ ). Electronic absorption data ( $CH_2Cl_2$  solution):  $\lambda_{max}$  264 nm ( $\epsilon$  56800  $M^{-1} cm^{-1}$ ), 285 nm ( $\epsilon$  54500  $M^{-1} cm^{-1}$ ), 422 nm ( $\epsilon$  8700  $M^{-1} cm^{-1}$ ), 605 nm ( $\epsilon$  18100  $M^{-1} cm^{-1}$ ).

**$[Pt(SCH_2CH_2NH_2)\{Ru(Bu_2sq)(dmsO)\}(btpyxa)](BF_4)_2$  (**[3]**-(**BF<sub>4</sub>**)<sub>2</sub>):** To a 2-methoxyethanol (8 mL) solution of complex **[1]**( $PF_6$ )<sub>2</sub> (45.8 mg, 0.028 mmol) was added an aqueous 0.1 M NaOH solution (2.8 mL, 0.28 mmol), and the mixture was stirred at room temperature for 2 h under  $N_2$ . The addition of an aqueous solution of  $NaBF_4$  to the solution caused dark-green solid to precipitate, which was collected by filtration. An aqueous solution of 0.1 M 2-aminoethanethiol hydrochloride (0.28 mL, 0.028 mmol), which was neutralized with an 0.1 M NaOH aqueous solution (0.28 mL, 0.028 mmol), was slowly added to a 2-methoxyethanol/water (8 mL/2 mL) solution of the dark-green solid. The reaction mixture was stirred at room temperature for another 21 h under  $N_2$ . Addition of a saturated aqueous solution of  $NaBF_4$  to the solution resulted in the precipitation of a dark-green solid, which was separated by centrifugation, washed with water and  $Et_2O$ , and dried in vacuo. Yield: 27.6 mg (0.017 mmol, 61%). Anal. Calcd for  $C_{71}H_{80}B_2F_8N_7O_4PtRuS_2 \cdot 2H_2O$ : C, 51.21; H, 5.08; N, 5.89%. Found: C, 51.38; H, 5.07; N, 5.80%. ESI-MS:  $m/z$  728 ( $[Pt(SCH_2CH_2NH_2)\{RuCl(Bu_2sq)\}(btpyxa)]^{2+}$ ). Electronic absorption data ( $CH_2Cl_2$  solution):  $\lambda_{max}$  277 nm ( $\epsilon$  53800  $M^{-1} cm^{-1}$ ), 309 nm ( $\epsilon$  48500  $M^{-1} cm^{-1}$ ), 467 nm ( $\epsilon$  7700  $M^{-1} cm^{-1}$ ), 743 nm ( $\epsilon$  6000  $M^{-1} cm^{-1}$ ). EPR (in MeOH, 293 K):  $g = 2.000$ .

**$[Pt(SCH_2CH_2NH_2)Ru(Bu_2sq)](btpyxa)(PF_6)_2$  (**[4]**( $PF_6$ )<sub>2</sub>):** To a 2-methoxyethanol/water (20 mL/10 mL) solution of complex **[2]**( $PF_6$ )<sub>2</sub> (53.8 mg, 0.032 mmol) was added an aqueous 0.1 M NaOH solution (3 mL, 0.3 mmol), and the mixture was stirred at room temperature for 14 h under  $N_2$ . Addition of an aqueous  $NH_4PF_6$  solution to the reaction mixture caused a purple solid to precipitate, which was collected with filtration. An aqueous solution of 0.1 M 2-aminoethanethiol hydrochloride (0.32 mL, 0.032 mmol), which was neutralized by an aqueous 0.1 M NaOH solution (0.32 mL, 0.032 mmol), was slowly added to the 2-methoxyethanol/water (10 mL/2 mL) solution of the purple solid. The reaction mixture was stirred at room temperature for another 14 h under  $N_2$ . Addition of a saturated aqueous solution of  $NH_4PF_6$  to the solution resulted in the precipitation of a dark-purple solid, which was separated by centrifugation, washed with water and  $Et_2O$ , and dried in vacuo. Yield: 33.3 mg (0.020 mmol, 63%).

Anal. Calcd for  $C_{69}H_{74}F_{12}N_7O_3P_2PtRuS \cdot 2H_2O$ : C, 48.65; H, 4.62; N, 5.76%. Found: C, 48.39; H, 4.63; N, 5.94%. ESI-MS:  $m/z$  689 ( $[Pt(SCH_2CH_2NH_2)Ru(Bu_2sq)](btpyxa)]^{2+}$ ). Electronic absorption data ( $CH_2Cl_2$  solution):  $\lambda_{max}$  278 nm ( $\epsilon$  54200  $M^{-1} cm^{-1}$ ), 316 nm ( $\epsilon$  41400  $M^{-1} cm^{-1}$ ), 520 nm ( $\epsilon$  5100  $M^{-1} cm^{-1}$ ), 857 nm ( $\epsilon$  9400  $M^{-1} cm^{-1}$ ). EPR (in MeOH, 293 K):  $g = 2.007$ .

**Elimination of DMSO.** A 2-methoxyethanolic solution (15 mL) of complex **[3]**( $PF_6$ )<sub>2</sub> (31.2 mg, 0.018 mmol) was heated at 100 °C for 19 h under  $N_2$ . The solution turned from dark green to dark purple in color. Addition of a saturated aqueous solution of  $NH_4PF_6$  to the solution resulted in the precipitation of complex **[4]**( $PF_6$ )<sub>2</sub>, which was separated by centrifugation, washed with water and  $Et_2O$ , and dried in vacuo. Yield: 22.6 mg (0.014 mmol, 76%).

**Physical Measurements.** ESI-MS spectra were measured with a Shimadzu LCMS-2010 liquid chromatograph mass spectrometer and a Waters Micromass LCT. Elemental analyses were carried out at the Research Center for Molecular-Scale Nanoscience, Institute for Molecular Science. Cyclic voltammetry (CV) was performed with an ALS/Chi model 660 electrochemical analyzer. Cyclic voltammograms were recorded at a scan rate of 100  $mV s^{-1}$  at room temperature using a glassy carbon working electrode, a Pt wire counter electrode and an  $Ag/Ag(NO_3)$  (0.01 mmol  $dm^{-3}$ ) reference electrode. All potentials were converted to SCE ( $E_{SCE} = E_{Ag/Ag^+} + 0.327 V$ ). Spectroelectrochemical measurements of UV-vis-NIR spectra were conducted using a thin-layer electrode cell with a platinum minigrid working electrode sandwiched between the two glass sides of an optical cell (path length 0.5 mm), a platinum counter electrode and an  $Ag/Ag(NO_3)$  reference electrode. A Hokuto Denko HA-501 potentiostat and a Shimadzu UV-3100PC UV-vis-NIR scanning spectrophotometer were used. EPR spectra were measured with a JEOL X-band spectrometer (JES-RE1XE). The  $g$  values were calibrated precisely by using an  $Mn^{2+}$  marker.

## References

- a) C. G. Pierpont, R. M. Buchanan, *Coord. Chem. Rev.* **1981**, 38, 45. b) C. G. Pierpont, C. W. Lange, *Prog. Inorg. Chem.* **1994**, 41, 331. c) C. G. Pierpont, *Coord. Chem. Rev.* **2001**, 216–217, 99. d) D. W. Michael, J. A. McCleverty, *J. Chem. Soc., Dalton Trans.* **2002**, 275.
- a) M. Kurihara, S. Daniele, K. Tsuge, H. Sugimoto, K. Tanaka, *Bull. Chem. Soc. Jpn.* **1998**, 71, 867. b) K. Tsuge, M. Kurihara, K. Tanaka, *Bull. Chem. Soc. Jpn.* **2000**, 73, 607. c) T. Wada, K. Tsuge, K. Tanaka, *Chem. Lett.* **2000**, 910. d) T. Fujihara, R. Okamura, T. Wada, K. Tanaka, *Dalton Trans.*, **2003**, 3221. e) T. Fujihara, T. Wada, K. Tanaka, *Dalton Trans.* **2004**, 645. f) T. Hino, T. Wada, T. Fujihara, K. Tanaka, *Chem. Lett.* **2004**, 33, 1596. g) T. Wada, K. Tanaka, *Eur. J. Inorg. Chem.* **2005**, 3832.
- a) K. Kobayashi, H. Ohtsu, T. Wada, K. Tanaka, *Chem. Lett.* **2002**, 868. b) K. Kobayashi, H. Ohtsu, T. Wada, T. Kato, K. Tanaka, *J. Am. Chem. Soc.* **2003**, 125, 6729.
- a) T. Wada, K. Tsuge, K. Tanaka, *Angew. Chem., Int. Ed. Engl.* **2000**, 39, 1479. b) T. Wada, K. Tsuge, K. Tanaka, *Inorg. Chem.* **2001**, 40, 329.
- R. Okamura, T. Wada, K. Aikawa, T. Nagata, K. Tanaka, *Inorg. Chem.* **2004**, 43, 7210.
- K. W. Jennette, J. T. Gill, J. A. Sadownik, S. J. Lippard, *J. Am. Chem. Soc.* **1976**, 98, 6159.

7 B.-C. Tzeng, W.-F. Fu, C.-M. Che, H.-Y. Chao, K.-K. Cheung, S.-M. Peng, *J. Chem. Soc., Dalton Trans.* **1999**, 1017.

8 H. Kurosaki, N. Yamakawa, M. Sumimoto, K. Kimura, M. Goto, *Bioorg. Med. Chem. Lett.* **2003**, *13*, 825.

9 a) J. M. Bevilacqua, J. A. Zuleta, R. Eisenberg, *Inorg. Chem.* **1993**, *32*, 3689. b) J. M. Bevilacqua, R. Eisenberg, *Inorg. Chem.* **1994**, *33*, 2913. c) S. D. Cummings, R. Eisenberg, *Inorg.*

*Chem.* **1995**, *34*, 2007. d) S. D. Cummings, R. Eisenberg, *J. Am. Chem. Soc.* **1996**, *118*, 1949. e) W. Paw, R. J. Lachicotte, R. Eisenberg, *Inorg. Chem.* **1998**, *37*, 4139.

10 J. A. Weinstein, N. N. Zheligovskaya, M. Y. Mel'nikov, F. Hartl, *J. Chem. Soc., Dalton Trans.* **1998**, 2459.

11 D. M. Duggan, D. N. Hendrickson, *Inorg. Chem.* **1975**, *14*, 955.